COMPUTATIONAL PREDICTION OF SHOT-PEENING INDUCED RESIDUAL STRESSES UNDER CYCLIC LOADING

J. Liu[a,b], H. Yuan[a]

[a]Dpt. of Mechanical Engineering, University of Wuppertal, 42119 Wuppertal, Germany
[b]School of Mech. & Vehicular Engineering, Beijing Institute of Technology, Beijing, China

ABSTRACT
The compressive residual stress induced by a shot peening process can be highly beneficial to fatigue performance of components. Experimental data reveal that the compressive residual stress can be relaxed and even be changed to detrimental tensile stress by mechanical loading. In this paper elastic-plastic finite element analysis as well as interactions between residual stress and applied mechanical loading are discussed. The stress-strain curves accounting for effects of shot peening are derived from tensile loading tests. With experimental verifications, a computational approach based on the experimental stress-strain curves and the empirical plastic strain profile is proposed for estimation of residual stress relaxation. The analysis shows a good agreement between measurement and computational prediction for tensile loading.

KEY WORDS
Residual stress relaxation; shot peening; finite element analysis; large plastic deformations

1. INTRODUCTION
Recently, experimental analysis [2] revealed that the compressive residual stresses near the specimen surfaces induced by shot peening can become tensile stresses after high tensile loading, especially for high peening intensities. This phenomenon is of particular interest, because it is not in accordance with the commonly held concept that no change from compressive to tensile residual stresses is observed in any of the specimens [1,6] and that the increase of surface roughness occurring due to the shot peening process should be responsible for the detrimental influence of shot peening on fatigue life in high loading conditions. Tensile residual stresses after high tensile loading levels definitely affect component life negatively. By far, the mechanism of presence of tensile residual stress has not been fully investigated and understood. Due to vanishing compressive residual stress, the life improvement diminishes. Computational analysis based on cyclic plasticity theory, however, does not predict such significant relaxation of residual stresses.

The present study is trying to clarify interaction of residual stresses based on experiments and computations. Due to extremely high plastic deformations in the shot peened surfaces, the material properties can generally not be covered by the usual tensile tests. In the present work we conducted special tensile tests with plastically pre-deformed specimens showing plastic strains up to 50% and used the resulting stress-strain curves to calibrate residual stress variations. Our computational results confirm that relaxation of residual stresses induced by shot peening at high level monotonic load for round bar

specimens can be predicted by FEM analysis accurately. This method can be applied for other specimens and materials.

2. EXPERIMENTS FOR LARGE PLASTIC DEFORMATIONS

In engineering applications the stress-strain relationship is approximated by the Ramberg-Osgood model

$$E\varepsilon = \sigma + \alpha\sigma^n \tag{1}$$

with *E* as Young's modulus, α as plastic offset parameter and n as plastic strain hardening exponent. The parameters of the Ramberg-Osgood model are usually taken from tensile tests. The plastic strain in engineering applications is limited to 1%. It follows that all parameters are identified based on these small plastic deformations.

For most structural components the mechanical loading varies with time. Therefore, one usually uses a cyclic plasticity model to analyze cyclic plastic deformations in the machine parts. A popular material model implemented in the commercial FEM code ABAQUS is the so-called combined hardening model with the yield surface defined by

$$F = \sigma_e\left(\sigma_{ij} - \alpha_{ij}\right) - \sigma_y = 0, \tag{2}$$

where $\sigma_e\left(\sigma_{ij} - \alpha_{ij}\right)$ is the Mises effective stress with respect to the back stress α_{ij}, and σ_y is the size of the yield surface. We assume associated plastic flow is expressed as

$$\dot{\varepsilon}_{ij}^p = \frac{\partial\sigma_e}{\partial\sigma_{ij}}\dot{\bar{\varepsilon}}^p, \tag{3}$$

where $\dot{\varepsilon}_{ij}^p$ represents the rate of plastic strain rate and $\dot{\bar{\varepsilon}}^p$ the equivalent plastic strain rate. The evolution law of this model consists of two components: a nonlinear kinematical hardening component, which describes the translation of the yield surface in stress space through the back stress, α_{ij}; and an isotropic hardening component, which describes the change of the equivalent stress defining the size of the yield surface, σ_y, as a function of the plastic deformation as

$$\sigma_y = \sigma_{y0} + Q\left(1 - exp\left(-b\bar{\varepsilon}^p\right)\right). \tag{4}$$

Obviously, growth of the yield surface depends only on $\dot{\bar{\varepsilon}}^p$, not on deformation components and deformation directions. For large equivalent plastic strain, σ_y approaches a constant value. Then, the stress-plastic strain hysteretic curve closes. In engineering materials one may find that the strain-controlled cyclic loading is characterized by tensile stress state, i.e. the loading ratio nearly equals 0. the accumulative cyclic plastic strain is not so large. The first loading amplitude defines essentially the maximum stress. The following plastic strain is rather small. Especially the shot peening induces high plastic deformations to the surface and the following mechanical loading will not exceed the initial plastic strain of shot peening.

To identify material parameters one has to perform cyclic tension and compression tests with significant plastic and reverse plastic deformations. In a strain controlled test the strain amplitude is symmetric about the stress axis which substantially differs from the loading history in a shot peened specimen.

In the shot peening process the specimen surfaces are loaded discontinuously in one direction of the stress space. The increasing deformations are dominated by compressive impacts. The huge plastic strains in the compressive residual stress layer are accumulated by many repeated shot impacts. Reverse plasticity does play a role in the shot peening process. Based on these considerations, one may assume that the loading history of the material layer below the shot is to be approximated by a monotonic loading path. Large plastic strains are reached by compressive deformations.

Analyzing stress variations in a shot peened specimen, one should assume that the stress state near the shot peened surface differs from the bulk material. The material in the compressive residual stresses zone is loaded by huge compressive plastic strain deformations, of up to 40% [7, 8, 11], which cannot be measured in tensile loading conditions. Much attention should be paid to the deformation behaviour of large-strain plasticity and also the stress-strain responses at small-scale re-yielding after large pre-strain [17]. Relaxation of the residual stress has to solve the following two problems: (1)

Effects of large plastic strains in a stress-strain relationship which are not measured in tension tests. (2) The difference of compressive stress and strain state from the tension states. For these reasons additional material tests are necessary to clarify residual stress evolutions in shot peened specimens.

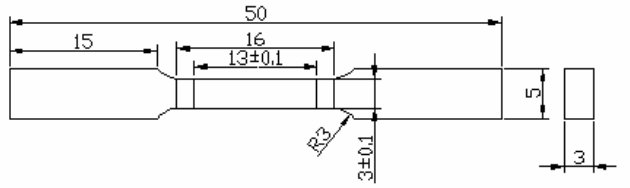

Fig. 2. The initial geometry of tensile specimens used in the present study (Unit: mm). The specimen thickness is reduced by 10-30% after uniaxial pressing to investigate effects of compressive plastic strains.

In order to understand the effect of large compressive plastic strains a series of specific tension specimens have been prepared and tested. The geometry of the tensile specimen is shown in Fig. 2. The initial specimen thickness is 3mm. The pre-strain is in the thickness direction of the specimens. To systematically study effects of pre-strain, the thickness of specimens is reduced to 90%, 80% and 70%, that is, the plastic strains are 10%, 20% and 30%, respectively. The pre-strains are induced by static uniaxial pressing. By neglecting friction in pressing, the deformations in specimens are uniaxial and uniform. After pressing the specimens are stress-free.
The specimens are tested under uniaxial elongation to fracture. The experimental records are summarized in Fig. 3 in which the horizontal axis denotes the equivalent plastic strain including initial compressive plastic strains. The vertical axis stands for the true stress calculated from the plastic volume-incompressibility. The experiments show clearly that the fracture strain depends on initial compressive strains. For large compressive pre-strain, the fracture strain increases significantly. On the other side, the plastic strain hardening does not vanish even beyond 30% plastic strain. Based on this conclusion we take a Ramberg-Osgood model for the whole relevant plastic strain regime.

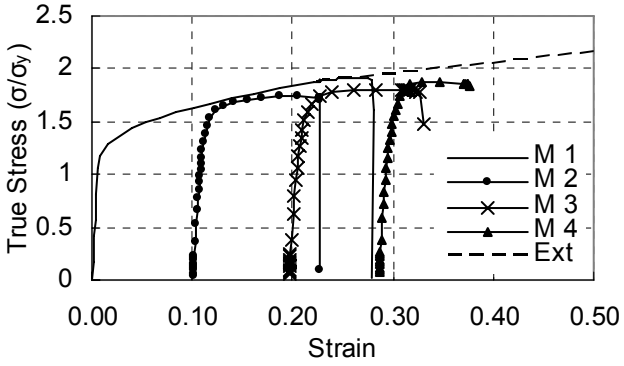

Fig. 3. Stress-strain curves for base material as well as pre-strained specimens (M 1: Base material specimen; M 2: 10% pre-strained specimen; M 3: 20% pre-strained specimen; M 4: 30% pre-strained specimen; Ext: The extended stress-strain curve for FEM computations.).

Based on the experimental data, the more realistic stress-strain relationship including large plastic deformations over 40% can be approximated by the Ramberg-Osgood model, as shown in Fig. 3. The model considers only monotonic loading or loads with minor cyclic stress variations. It is still open how to characterize stress behaviour for higher cyclic stress amplitudes. More detailed experimental investigations to this issue are needed for clarifying cyclic plastic features coupled with high pre-strains.
Since plastic strain hardening is significant in large strain regions, one expects that the residual plastic strains induced by shot peening may affect residual stress variations. Most published papers on this topic are based on computational simulations [4, 7]. Di-

rect measurement of the plastic strain seems not applicable at present. Predictions of residual strain distribution are assumed to be described in the following section.

3. VARIATIONS OF RESIDUAL PLASTIC STRAINS

The common generalized form of plastic strain induced by shot peening is summarized in Fig. 4. The distribution of residual strain is written as

$$\bar{\varepsilon}^{pl} = \varepsilon_0 \left(1 - \frac{x}{x_0}\right)^n \exp\left(\alpha \left(1 - \frac{x}{x_0}\right)^{n+1} - 1\right) \tag{5}$$

with four parameters: x_0 the depth with vanishing plastic strain, ε_0 the plastic strain at the surface (x=0), α is a parameter for non-monotonic variations of plastic strain. The exponent n describes variations.

Parameter study is executed to understand the general trend about dependence of residual stress variations on these parameters. Shot peening generates high plastic strain (up to 30–40%) [9, 11]. Thus, the plastic strain at surface, i.e. ε_0, ranges from 0.3 to 0.4. In this study, the depth of plastic strain x_0 is taken as same as the initial depth of compressive residual stress.

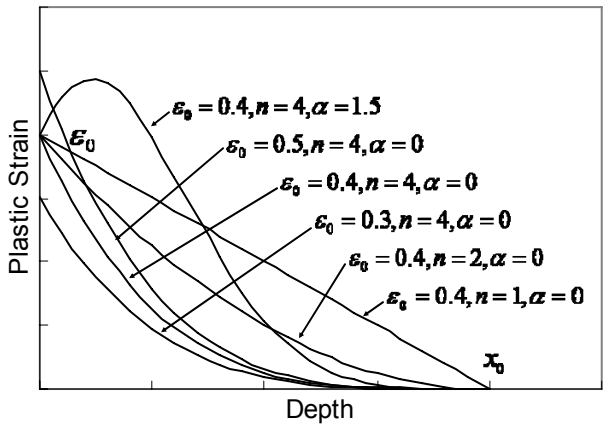

Fig. 4. Initial computational plastic strain distributions.

In literature one often finds two very different distributions: monotonic decreasing variation and distribution with maximum under the surface. Both types can be approximated by Equation (5). In our computations the various plastic strain distributions will be discussed.

4. COMPUTATIONAL PREDICTIONS OF RESIDUAL STRESS RELAXATIONS

4.1 Residual stress variations based on cyclic plasticity

The commercial finite element program ABAQUS has been used for the present study. We consider a uniaxial tensile bar which can be modeled using axisymmetric elements. Loads are applied by a uniform displacement along the axial direction. The material behaviour is described by the combined hardening model, Eq. (3).

As initial conditions, both residual stresses and equivalent plastic strains are assigned to integration points as a function of the distance from the free surface. The initial backstress in the constitutive equation has been assumed based on impact simulations. In Fig. 5 the residual stress variations at the initial state, after 0.7% and 1.2% elongation are summarized. The initial residual stress profile agrees with experimental records [2]. After one cycle of static loading, the residual stress profile changes due to new plasticification in the whole specimen. The computation predicts evolutions of residual stress up to 0.7% elongation at which the new plastic deformation in the specimen does not affect the residual stresses near the specimen surface. Significant deviations from experimental data [2] are observed in loading beyond 1% elongation. Whereas the experiment [2] shows tensile residual stress at the specimen surface, the computation

based on the combined hardening model predict vanishing residual stress. Fig. 6 plots the residual stress at the specimen surface as a function of applied loading elongation. The computational results deviate from experimental data only at high loading levels. Whereas the experiment [2] shows a linear increment of residual stress, the computation approaches to zero.

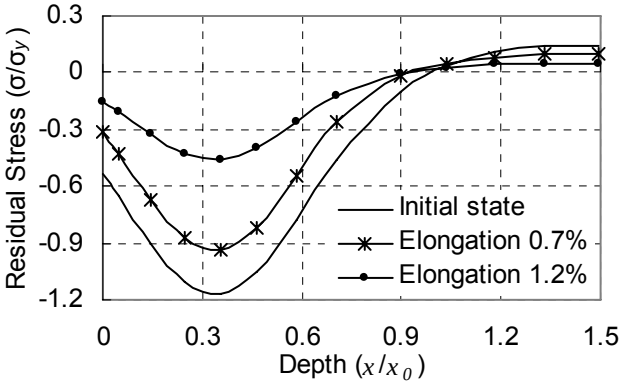

Fig. 5. FEM computational residual stress profiles based on conventional cyclic plasticity model.

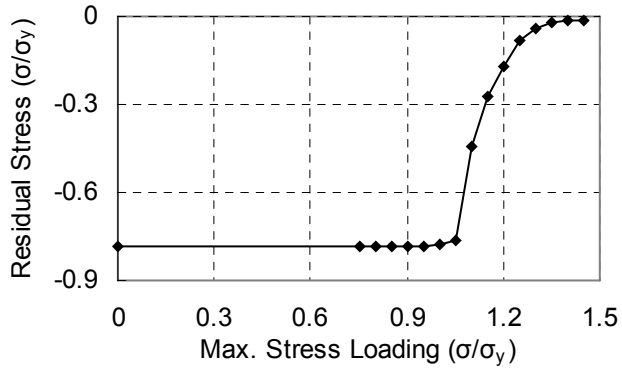

Fig. 6. Variations of FEM computational residual stress on the surface based on conventional cyclic plasticity model. The computational results are hardly affected by the initial plastic strain profiles.

Such computational results are obvious if the material behaviour is approximated as being elastic-perfectly plastic. As soon as the whole specimen is plastified, the upper and lower stresses are described by the yield stress. Under pulsating loading condition, the lower stress is zero. In cyclic plasticity, plastic strain hardening vanishes for a large amount of plastic deformation. It follows that the residual stress diminishes for large elongations. The deviation implies that one may not use the conventional cyclic plasticity model to calibrate the residual stress variation in the shot peened specimen. The plastic strain distribution does not effect residual stress prediction since the incremental stress-strain relation becomes independent of plastic strain.

4.2 Residual stress variations based on multi-layer model

Shot peening changes material properties below the specimen surface. However, material properties in the material are not homogeneous due to gradually varying plastic straining as shown in Fig. 2. The material on the specimen surface is changed most strongly, the material at the depth where compressive residual stresses approach zero may be assumed not to be affected. In computations this inhomogeneous material can be approached by a multi-layered model.

In the multi-layered model we assume that only the yield stress varies from layer to layer. It will certainly cause discontinuity in the material property, but becomes increasingly accurate with layer number. Due to varying plastic strains in the specimen surface, the yield stress reaches its maximum in the material layer below the specimen surface. The stress difference is proportional to the final tensile residual stress. In Fig. 7 and Fig. 8

computational results are plotted. Due to the small discontinuity in the material property the residual stress profiles near the specimen surface show small vibrations. The residual stress variations are corresponding to experimental data [2] in total. The tensile residual stress near the specimen surface is a direct consequence of yield stress increment. It implies that the higher tensile residual stress at higher loading cannot be approached based on the proposed multi-layer model.

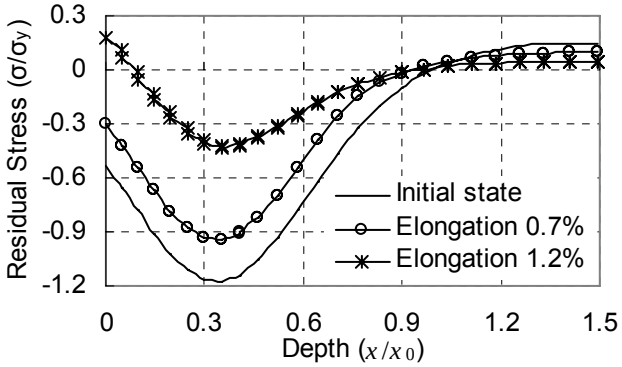

Fig. 7. FEM computational residual stress profiles based on the multilayer model. The computation predicts realistic variations of the residual stress in comparing with known experiments [2].

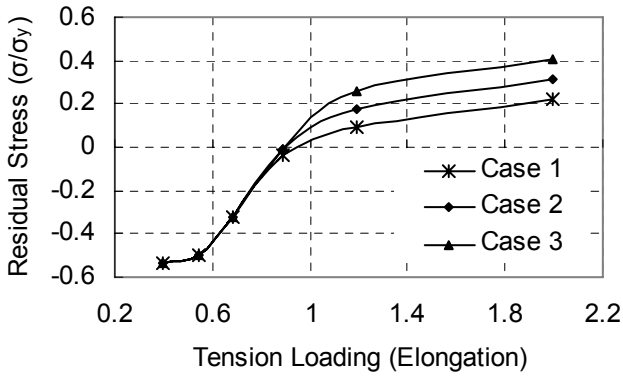

Fig. 8. Variations of FEM computational residual stress based on multilayer model (In Case 1, 2 and 3, the yield stresses of material on surface are $1.3\sigma_y$, $1.4\sigma_y$ and $1.5\sigma_y$, respectively. σ_y is yield stress of the bulk material.).

4.3 Residual stress variations based on compressive stress-strain curves

The previous results show strong effects of plastic strain hardening. Zero hardening will not generate high tensile residual stresses. Based on the experimental tension tests, we are able to use the monotonic stress-strain curve for the residual stress evolution analysis. Only the initial plastic strain has to be assumed in accordance.

Fig. 9 shows the residual stress values on the specimen surface for various plastic strain model (5) with α=0. For a given ε_0, the residual stress variation depends on n slightly. ε_0 plays a more important role in residual stresses near the specimen surface than n does, as shown in Fig. 9.

In Figure 10 results of two loading levels combined with three exponents n in Eq. (5) are summarized. Whereas n>1 shows continuous gradient of plastic strain profile, n=1 means a jump in the gradient. At low loading levels, the discontinuity in plastic strain gradient seems change RS. Up to 0.7% elongation, the plastification in the bulk specimen is not so large, so that the residual stress zone is changed significantly. It follows that the plastic strain distribution does not effect residual stress variations. For large applied loading, e.g. 1.2% elongation in Fig. 10, n dos not affect the residual stress variations.

The significant deviations as residual stress approaches zero results from the sensitive relation between plastic strain and strain hardening. Most deviations are observed in

n=1, i.e. linear plastic strain distributions. With increasing *n*, the residual stress profile becomes smooth. One may conclude that the *n* should be larger than 2 and its effects are negligible.
Additional computations show that α controls the residual stress profile only at large applied loading in the same way as parameter *n*.

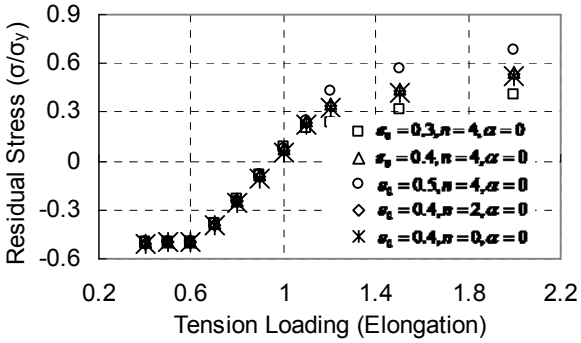

Fig. 9. Computational predictions of residual stress variations near specimen surface based on various plastic strain distributions.

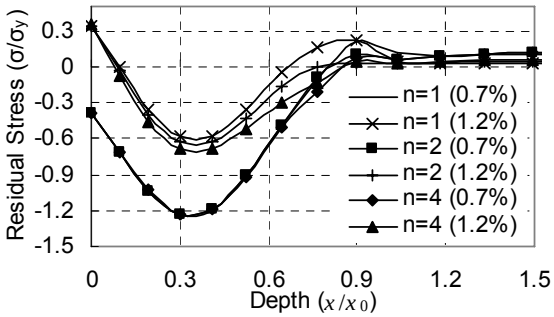

Fig. 10. Residual stress profiles affected by plastic strain distributions (ε_0=0.4, α=0, Tension loading is elongation in percentage).

5. CONCLUSIONS

In this paper residual stress relaxation models were proposed based on an assumed initial plastic strain profile. The models were verified using finite element analysis with experimental data [2]. Based on extensive FE computations we may conclude:

1. Cyclic plastic stress-strain relationship contains too low strain-hardening and can not simulate the effects of large plastic deformations. The predicted residual stress near the specimen surface have to approach zero which does not match experiments of shot peened specimens
2. Shot peening changes material properties of the compressive zone. The stress-strain relationship has to be identified based on pre-strained specimens. The peened material exhibits significantly more plastic strain hardening, especially in large deformation regions.
3. The tensile residual stress after high mechanical loading can be predicted based on stress-strain relationship taken from pre-strained specimens. Our computations agree with known experimental data reasonably. Based on this knowledge, one may further simplify residual stress variations by using a simple monotonic stress-strain curve.
4. Effects of cyclic loading have to be investigated separately. It remains open how to calibrate cyclic softening of the material at such high plastic strains. This work needs very detailed and specific defined experiments.

ACKNOWLEDGMENTS

The authors gratefully acknowledge experimental evidence from Dipl.-Ing. Jürgen Hoffmeister of University of Karlsruhe as well as experimental support of Dr. Liao Ridong of Beijing Institute of Technology, PR China. The project is financed by MTU Aero Engines in the frame of LuFo-3 of BMWi.

REFERENCES

[1] Guechichi H, Castex L, Fatigue limits prediction of surface treated materials, J. Mater. Process Tech. 172 (2006) 381-387.

[2] Hoffmeister, J., et al. Work in progress. Research project of MTU / University of Karlsruhe

[3] Kobayashi M, Matsui T, Murakami Y. Mechanism of creation of compressive residual stress by shot peening, Int. J. Fatigue 20 (5) (1998) 351-357.

[4] Meguid SA, Shagal G, Stranart JC, 3D FE analysis of peening of strain-rate sensitive materials using multiple impingement model, Int. J. Impact Eng. 27 (2002) 119-134.
[5] Ochi Y, Masaki K, Matsumura T, Sekino T. Effect of shot-peening treatment on high cycle fatigue property of ductile cast iron. Int. J. Fatigue 23 (2001) 441-448.
[6] de los Rios ER, Walley A, Milan MT, Hammersley G, Fatigue crack initiation and propagation on shot-peened surfaces in A316 stainless steel. Int. J. Fatigue 17 (7) (1995) 493-499.
[7] Sridhar BR, Nafde WG, Padmanabhan KA, Effect of shot peening on the residual stress distribution in two commercial titanium alloys, J. Mater. Sci. 27 (1992) 5783-5788.
[8] Torres MAS, Voorwald HJC, An evaluation of shot peening, residual stress and stress relaxation on the fatigue life of AISI 4340 steel, Int. J. Fatigue 24 (2002) 877-886.
[9] Webster GA, Ezeilo AN. Residual stress distributions and their influence on fatigue lifetimes, Int. J. Fatigue 23 (2001) s375-s383.
[10] Yoshida F, Uemori T, A model of large-strain cyclic plasticity describing the Baushinger effect and workhardening stagnation, Int. J. Plasticity 18 (2002) 661-686.
[11] Zhuang WZ, Halford GR. Investigation of residual stress relaxation under cyclic load, Int. J. Fatigue 23 (2001) s31-s37.